Petrophysics of Core Plugs from CRP-2A Drillhole, Victoria Land Basin, Antarctica

J.D. BRINK & R.D. JARRARD

Department of Geology & Geophysics, 717 WBB, Univ. of Utah 135 S. 1460 East, Salt Lake City UT 84112-0111 - USA

Corresponding author (jarrard@mail.mines.utah.edu)

Abstract - A suite of petrophysical measurements - velocity versus pressure, bulk density, porosity, matrix density, and magnetic susceptibility – was undertaken on 63 core plugs from CRP-2A. These data are used to calibrate neutron, resistivity, and magnetic susceptibility well logs. Agreement between core-plug magnetic susceptibility measurements and both well-log and whole-core data is excellent. Comparison of core-plug bulk densities with continuous well-log density records shows very good agreement. Core-plug measurements of matrix density permit conversion of the well-log and whole-core density records to porosity. Sands and muds exhibit similar downhole compaction patterns, and both patterns are consistent with 250 ± 150 m of exhumation. Pervasive cementation, particularly in the lower half of the hole, has affected many CRP-2A petrophysical parameters: (1) fractional porosities are reduced by about 0.05 – 0.10 in the lower part of the hole; (2) velocity and porosity rebound are much smaller than is usually observed for unconsolidated sediments with burial depths similar to CRP-2A; (3) velocities are unusually insensitive to pressure, suggesting that any exhumation-induced microcracks have been sealed subsequently; (4) the velocity/porosity relationship lacks the characteristic signature of exhumation-induced microcracks; (5) the velocity/porosity relationship changes with depth, indicating downhole increase in consolidation; (6) Vp/Vs ratios of the highest-porosity sediments are unusually low, implying enhancement of framework stiffness.
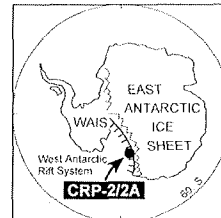
INTRODUCTION

The Cape Roberts Project (CRP) is an international drilling project whose aim is to reconstruct Neogene to Palaeogene palaeoclimate by obtaining continuous cores and well logs from a site near Cape Roberts, Antarctica. The first CRP drillhole, CRP-1, cored 148 m of Quaternary and Miocene sediments (Cape Roberts Science Team, 1998). The second CRP drillhole, CRP-2/2A, extended to 624 mbsf (metres below sea floor) with an average 94% recovery of Oligocene to Quaternary sediments (Cape Roberts Science Team, 1999). Continuous well-log measurements were made throughout most of CRP-2/2A.

Seismic velocity, density, and porosity of sediments drilled by the CRP can be determined in three ways: by whole-core measurements, by downhole logging, or by lab measurements on core plugs. Continuous whole-core measurements of bulk density, compressional wave velocity (V_p), and magnetic susceptibility were made at the rig site (Cape Roberts Science Team, 1999; Niessen et al., this volume). Well-log measurements of density, neutron porosity, resistivity, V_p, magnetic susceptibility, and natural gamma radiation were obtained at the rig site (Cape Roberts Science Team, 1999); revised and calibrated results are developed later in this chapter and used in the stratigraphic interpretations of Brink et al. (this volume).

This study provides the third, complementary, data set: laboratory measurements of velocity versus pressure and of bulk density, porosity, matrix density, and magnetic susceptibility for 63 core plugs. All major lithologies present in the CRP-2A cores were sampled for this study: diamictites, sandstones, and mudstones. Although core-plug measurements are made on samples of different volumes and with different methods from whole-core and well-logging data, they can address issues critical to the analysis and interpretation of the well-log and whole-core measurements. These issues are:

1- Core-plug measurements can be used to calibrate density, neutron, resistivity, velocity, and magnetic susceptibility well logs and to confirm the calibration of whole-core measurements.

2 - Do core-plug petrophysical measurements - particularly of velocity - detect diagenetic effects?

3 - What is the matrix density of the CRP-2A sediments? Matrix density is needed for conversion of well-log and whole-core densities to porosities.

4 - Measurements of seismic velocity versus pressure indicate how different *in situ* velocities are from whole-core measurements made at laboratory pressure.

METHODS

In McMurdo Station, Antarctica, 63 cylindrical samples were drilled from the working halves of the CRP-2A cores; the circulating fluid used to remove cuttings was water. Sample diameters were 2.5 cm. Volumes of most samples were 10-12 cm^3, but seven samples were only 1-8 cm^3. All samples analyzed were Oligocene to Quaternary in age. Some Quaternary and shallow Miocene samples were too unconsolidated to drill, so four samples were obtained with a square plastic container. The semiconsolidated nature of these four samples prevented petrophysical measurements beyond magnetic suscepti-

bility. Shortly after sampling, palaeomagnetic measurements were undertaken on most samples. These measurements included remanence, alternating field demagnetization, and magnetic susceptibility (Cape Roberts Science Team, 1999). The magnetic susceptibility of the samples was later remeasured at the University of Utah, using a KLY-2 Kappa bridge rather than the less sensitive Bartington instrument used for the original measurements (Tab. 1).

Analyses of CRP-1 sediments demonstrated that resaturating samples in seawater caused degradation of some sediments (Brink & Jarrard, 1998). Most CRP-1 and CRP-2A sediments contain some smectite (Ehrmann, 1998, this volume), and exposure of smectite-bearing sediments to water can cause clay swelling and associated spalling. Consequently, we evacuated the remaining water from all core-plug samples and used kerosene as the saturating fluid, rather than seawater. Kerosene is often used in the petroleum industry for core-plug drilling and petrophysical measurements, because it does not adversely affect the integrity of shale-rich sediments.

Porosity, bulk density, and matrix density of the core plugs (Tab. 1) were determined using a simple weight-and-volume technique, as described by Brink & Jarrard (1998) and Brink (1999). Accuracy of this technique was confirmed by measuring a suite of standard samples. These standards are Ferron sandstones that had previously been measured by Amoco, using a helium porosimeter and mercury immersion, as described by Sondergeld & Rai (1993).

Grain size analysis was performed on disaggregated 1-g subsamples of six CRP-2A samples, using a Microtrac laser grain size analyzer. A dispersant was employed to prevent clumping of clay minerals. Table 2 lists sample depth, lithology, and the 10 and 50 percentiles of grain sizes.

Velocities of kerosene-saturated samples were measured in a New England Research velocimeter, as described by Brink & Jarrard (1998) and Brink (1999). Pore pressures were atmospheric, so confining pressure was equal to differential pressure. The velocimeter accuracy was confirmed by replication of Amoco results on Ferron sandstone samples, for both compressional wave velocity (V_p) and shear wave velocity (V_s) and for both saturated and dry states. Results are shown in table 3. One third of the samples was unsuitable for velocity measurement, due to non-cylindrical shape, cracks, or insufficient length.

Because the fluid bulk modulus of seawater (2.4 GPa) is almost double that of kerosene (1.3 GPa), Brink & Jarrard (1998) used the Gassmann (1951) equation to convert measured velocities of kerosene-saturated CRP-1 samples to those of seawater-saturated samples. This correction indicated that water-saturated velocities are 6-18%, or 150-340 m/s, higher than kerosene-saturated velocities. We found, however, that kerosene-saturated and water-saturated velocities for our Ferron standards agreed, to within about 1%. Furthermore, as described later, the CRP-2A kerosene-saturated velocities are in reasonable agreement with log velocities, whereas application of the Gassmann equation to the core plug velocities causes them to be much faster than expected. Because the Gassmann equation appears to overestimate

Tab. 1 - Petrophysical measurements on CRP-2A core plug samples.

Depth (mbsf)	Density (kg/m³)	Porosity (fractional)	Matrix Density (kg/m³)	Vol. Mag. Susc. (μ SI)
65.77	2072	0.379	2725	2812
70.85	1940	0.421	2624	2313
83-1	2361	0.298	2939	
83-2	2416	0.249	2884	
87.68				2295
97.00	2489	0.138	2728	3219
107.45	2103	0.249	2468	3082
115.76	2022	0.398	2697	4302
124.59	2305	0.248	2736	2734
130.67	2121	0.330	2673	3601
139.65	2033	0.387	2685	2052
148.75	2052	0.419	2812	1104
153.46	2096	0.375	2753	1298
161.32	2038	0.405	2744	1670
169.35	2073	0.397	2781	2866
181.05	2002	0.429	2755	2544
203.37	2233	0.289	2734	1369
211.13	2138	0.336	2715	1676
219.34	2169	0.336	2761	1716
232.10	2104	0.352	2704	1601
239.40	2222	0.301	2748	2204
251.03	2072	0.372	2708	1090
259.53	1849	0.432	2495	103
268.14	2077	0.369	2707	
280.37	2647	0.286	3307	227
294.67	2114	0.339	2684	
301.68	2286	0.263	2745	477
308.41	2217	0.334	2827	222
312.88	2003	0.399	2667	176
321.42	2107	0.368	2752	227
322.41	2088	0.380	2754	246
330.50	2119	0.350	2721	944
336.60	2192	0.445	3147	1041
344.65	2089	0.348	2669	1286
352.32	2299	0.258	2751	2170
357.85	2227	0.259	2655	1177
366.10	2335	0.213	2697	
376.00	2544	0.099	2715	482
382.10	2234	0.293	2747	195
383.80	2276	0.255	2714	
394.52	2293	0.267	2763	190
401.52	2686	0.043	2761	
405.30	2357	0.213	2724	661
409.25	2293	0.189	2595	830
414.13	2350	0.225	2743	1164
437.36	2294	0.243	2709	1085
445.43	2066	0.364	2678	1824
452.75	1993	0.394	2639	1605
458.53	1988	0.425	2718	1298
468.27	2024	0.380	2652	968
478.14	2156	0.331	2728	239
484.96	2161	0.341	2762	323
490.65	2410	0.205	2773	1988
499.73	2226	0.262	2660	2130
507.60	2197	0.266	2631	359
509.17	2145	0.298	2630	122
541.70	2232	0.278	2706	1355
556.45	2207	0.255	2620	
565.39	2210	0.303	2736	1498
582.30	2342	0.245	2777	
589.43	2285	0.227	2662	
598.71	2185	0.231	2542	103
608.46	2301	0.214	2655	1072
618.14	2258	0.285	2761	85
624.10	2339	0.190	2652	2167

Tab. 2 - Grain size analysis of 6 CRP-2A core plugs, in μm.

Depth (mbsf)	Lithology	50% Grain Size	10% Grain Size
65.77	Silt	7.51	2.56
211.13	Sandy-Silt	15.81	2.86
232.1	Silt	11.09	2.92
452.75	Silt	9.43	2.78
458.53	Silt	5.47	2.23
478.14	Silt	8.36	2.73

Tab. 3 - Velocity measurements on core plugs.

Depth (mbsf)	Pressure (MPa)	V_p (km/s)	V_s (km/s)	V_p/V_s	in situ Pressure (MPa)	Meas. Pressure (MPa)	V_p (km/s)	V_s (km/s)	V_p/V_s
65.77					0.66	1.73	1.91	1.02	1.88
70.85					0.71	2.76	1.55	1.05	1.49
115.76	0	1.97	1.02	1.93	1.17	1.73	1.99	1.04	1.92
139.65	0	2.16	1.15	1.87	1.42	1.38	2.16	1.16	1.87
148.75	0.69	2.28	1.22	1.82	1.51	1.55	2.28	1.22	1.83
153.46		2.32			1.56	1.55	2.38	1.36	1.75
161.32	0	2.30	1.28	1.79	1.64	1.73	2.31	1.37	1.69
169.35	0.69	2.07			1.72	1.73	2.08		
181.05	0.69	1.86	0.94	1.98	1.84	1.86	1.86	0.94	1.97
211.13	2.07	1.97			2.15	2.07	2.01		
232.10	0	2.04	1.08	1.89	2.36	2.42	2.10	1.13	1.86
251.03	0	1.94	0.98	1.97	2.56	2.55	2.11	1.07	1.98
259.53	0	2.03	1.07	1.89	2.64	2.62	2.04	1.08	1.89
268.14	0	2.22	0.99	2.24	2.73	2.76	2.24	1.02	2.20
301.68	0.69	2.99	1.71	1.75	3.07	3.11	3.01	1.72	1.75
321.42	0.69	2.05	0.98	2.09	3.27	3.45	2.13	1.01	2.11
322.41	0	2.07	0.97	2.13	3.28	3.28	2.11	1.03	2.04
330.50	0	2.72	1.51	1.96	3.37	3.45	2.73	1.52	1.87
336.60	0	2.59			3.43	3.45	2.68	1.35	1.99
344.65	0	2.62	1.45	1.80	3.51	3.45	2.64	1.49	1.77
352.32	0	2.65	1.32	2.01	3.59	3.59	2.68	1.33	2.01
357.85	0	2.82	1.43	2.00	3.65	3.66	2.82	1.42	1.98
382.10	0	2.71	1.59	1.71	3.89	3.86	2.73	1.59	1.71
394.52	0	2.74	1.60	1.71	4.02	4.00	2.85	1.68	1.70
401.52	0	5.02	2.41	2.08	4.09	4.14	5.12	2.86	1.79
414.13	0	2.86	1.63	1.75	4.22	4.14	2.95	1.68	1.76
437.36	0	3.04	1.79	1.69	4.46	3.45	3.06	1.81	1.70
452.75	0	2.40	1.32	1.81	4.61	4.66	2.40	1.31	1.83
458.53	0	2.30	1.24	1.86	4.67	4.62	2.34	1.23	1.89
468.27	0	2.42	1.33	1.81	4.77	3.45	2.47	1.35	1.83
478.14	0	2.41	1.36	1.78	4.87	4.14	2.46	1.38	1.78
484.96	0.69	2.02	0.83	2.44	4.94	4.93	2.04	0.83	2.45
490.65	0	3.60	1.77	2.04	5.00	5.18	3.73	1.80	2.08
499.73	0	2.79	1.70	1.64	5.09	5.18	2.96	1.67	1.74
507.60	0	2.66	1.17	2.28	5.17	5.18	2.75		
509.17	0	2.36	0.96	2.47	5.19	5.18	2.45	0.97	2.52
541.70	0	2.85	1.62	1.76	5.52	5.52	2.87	1.65	1.74
556.45	0.69	2.39	1.45	1.65	5.67	6.90	2.70	1.52	1.78
565.39	0	2.76			5.76	5.73	2.78	1.56	1.78
582.30	0	3.43	1.78	1.93	5.98	5.93	3.52	2.10	1.68
598.71	0	3.82	2.33	1.64	6.10	6.07	3.87	2.40	1.61
624.10	0	3.67	2.13	1.72	6.36	6.35	3.67	2.17	1.69

the difference between kerosene-saturated and water-saturated velocities, we did not apply it to our velocities. The reason for this surprising similarity of water-saturated and kerosene-saturated velocities is not known; it may be a manifestation of shear weakening, a recently discovered phenomenon in rocks containing illite (G. Boitnott, personal communication, 1999). Illite is pervasive within CRP-2/2A (Ehrmann, this volume).

RESULTS

CORE PLUG CALIBRATION OF WELL LOGS

Drilling of the 624-m CRP-2/2A hole included three periods of downhole logging (Cape Roberts Science Team, 1999). The raw data collected by most logging tools require calibration. For example, the density tool, which determines bulk density by measuring gamma-ray attenuation, was calibrated by comparison to whole-core densities (Bücker et al., this volume). We converted the density log to a porosity log by assuming a constant matrix density and applying the following relationship:

$$\rho_b = \phi\rho_f + (1-\phi)\rho_{ma}$$

where ρ_b is bulk density, ϕ is fractional porosity, ρ_f is fluid density, and ρ_{ma} is matrix density. CRP-2A matrix densities (Tab. 1) have a mean value of 2720 kg/m^3, consistent with the mean of 2700 kg/m^3 measured for CRP-1 (Brink & Jarrard, 1998). The low standard deviation of measured matrix densities (120 kg/m^3) and lack of detectable lithologic effects indicate that the assumption of uniform matrix density introduces only minor errors into the conversion from density to porosity.

The CRP-2A shallow resistivity log contains the most detailed character of the three resistivity curves and demonstrates negligible influence from conductive borehole fluids. Shallow resistivity was converted to formation factor to eliminate the effect of pore water conductivity:

$$FF = R_o / R_w$$

where FF is formation factor, R_o is formation resistivity, and R_w is pore fluid resistivity. Changes in pore fluid resistivity versus depth were determined by calculating R_w from a temperature log and seawater salinity. This formation factor log was calibrated to porosity by crossplotting the natural logarithm of core plug porosity versus the natural logarithm of formation factor log at equivalent depths. The crossplot excludes data for clay lithologies to avoid possible effects of clay conduction. Linear regression demonstrates a high correlation coefficient and provides an equation (Tab. 4) that can be used to convert the FF log to a porosity log. A microresistivity log, extracted from dipmeter data by Jarrard et al. (this volume), was similarly converted to FF and then to porosity (Tab. 4).

Raw counts from the neutron-porosity log were compared to both core plugs and the calibrated density-porosity log. Only density values from the open-hole

Tab. 4 - Calibration of well logs based on regression analysis.

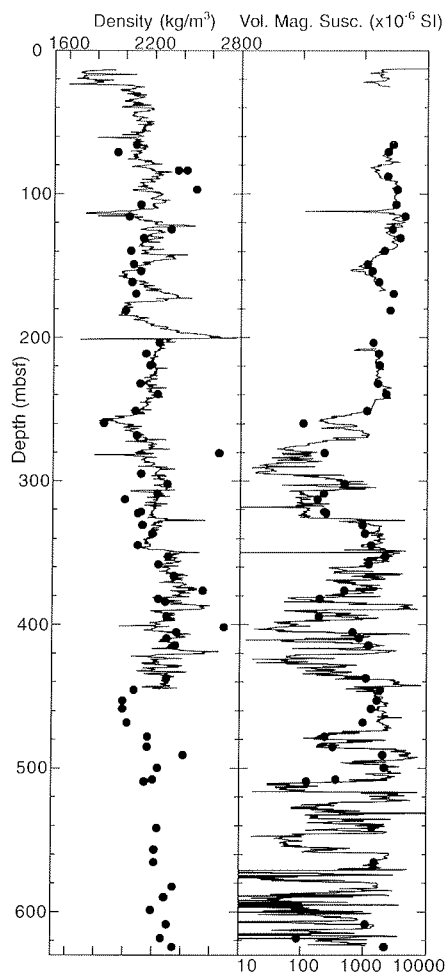| Standard (Y)	Log (X)	Regression Equation	Correlation Coefficient (R)
Core-Plug Porosity	Neutron counts	Y = 0.437 - 0.0186X	0.833
Density Porosity	Neutron counts	Y = 0.467 - 0.0226X	0.661
Core-Plug Porosity	Resistivity Formation Factor	Y = 10.52 - 2.35X	0.707
Core-Plug Porosity	Dipmeter Formation Factor	Y = 9.28 - 1.80X	0.634
Core-Plug Mag Susc	Magnetic Susceptibility	Y = -128 + 57.6X	0.929

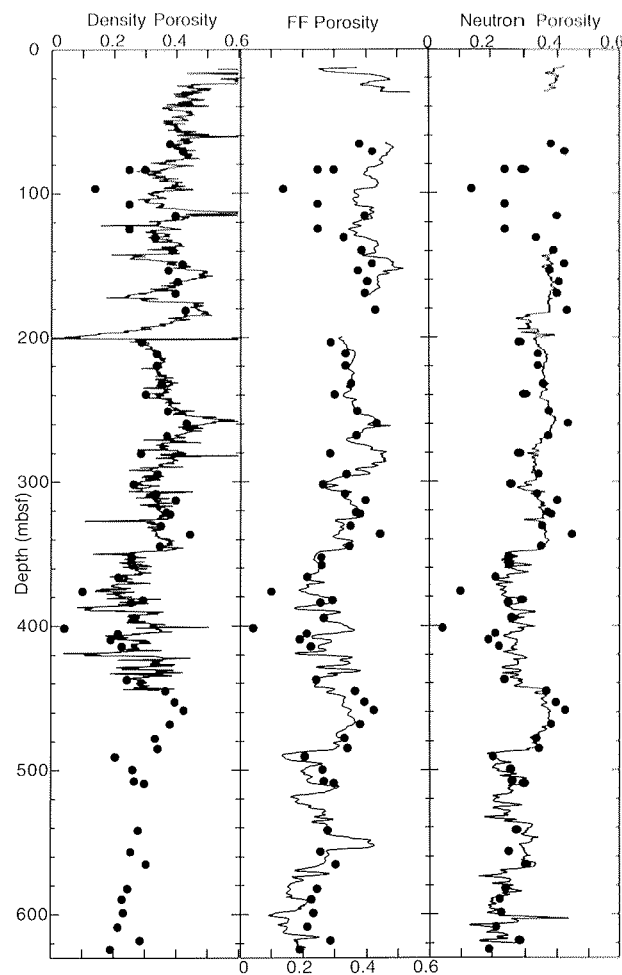*Fig. 1* - Density and magnetic susceptibility logs, compared to core-plug values.

Fig. 2 - Comparison of core-plug porosities to porosity logs. Density, formation-factor, and neutron logs were converted to porosity using the core-plug calibrations of table 4.

logged portion (200 – 440 mbsf) were used in the regression analysis. Both well-log and core-plug calibration of the neutron log excluded clay dominated lithologies which may give anomalously high neutron values due to bound water in clay minerals. Regression analysis indicates that the neutron values are more highly correlated to core plug porosities than to log densities (Tab. 4), despite the fact that core-plug volumes are much smaller and less representative than density and neutron log volumes. Therefore the final neutron porosity log is based on core-plug calibration.

POROSITY, BULK DENSITY, AND MATRIX DENSITY

Log measurements of bulk density are compared to core-plug bulk densities in figure 1. Despite the larger sampled volume for well-log measurements than for core plugs, the overall pattern is clearly one of very good agreement between the two measurement techniques. This consistency confirms the general accuracy of the density log. Consistency is better for the open-hole (below 200 mbsf), because accurate borehole compensation is not feasible for through-pipe density logs.

Figure 2 compares core-plug porosities to three core-plug calibrated porosity logs. Microresistivity-based

porosity, not shown, is similar to FF-based porosity except for higher vertical resolution. Anomalously low core-plug porosity values at 402 and 376 mbsf are caused by locally intense cementation. Lower core-plug porosities than log porosities in the interval 80 – 120 mbsf may be due to diamict heterogeneity. Some differences between neutron-porosity and core-plug porosities may be attributable to bound water in clay minerals, which increases apparent porosity in the neutron log. However, the neutron log has the best agreement of all the porosity logs with core-plug porosities (Fig. 2; Tab. 4). The FF-based porosity log may also overestimate porosity in clay-rich zones, due to clay conduction. In high-porosity sediments such as these, however, the influence of clays on pore tortuosity counteracts that of clay conduction (Erickson & Jarrard, 1998a). We observe no detectable difference between sand and mud patterns on a porosity/FF crossplot for CRP-2A. Density porosity values may diverge from core-plug porosities when an incorrect matrix density is assumed, when casing attenuation affects density log values, or when borehole washouts cause the density log to read anomalously low values.

Comparisons of the six grain size analyses (Tab. 2) to matrix density, velocity, and magnetic susceptibility values show no correlation. However, core-plug grain size does
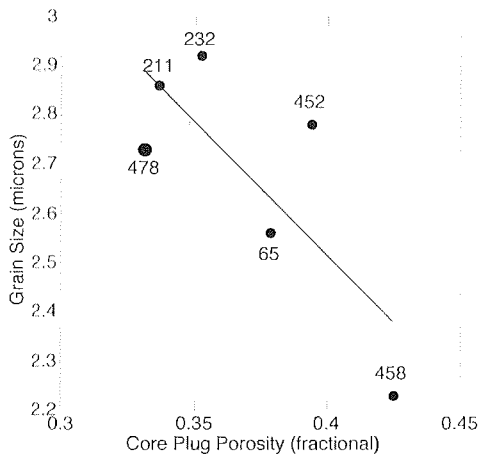
Fig. 3 - Tenth-percentile grain size of six selected samples is correlated with porosity; the regression line shown has a correlation coefficient R=0.77. In contrast, no correlation between depth (numbers adjacent to points) and porosity is evident for these data.

correlate with porosity and density. Figure 3 is a crossplot of 10-percentile grain size versus porosity. This relationship, although based on a small subset of CRP-2A, suggests that increased clay fraction (decreased 10-percentile grain size) increases porosity.

MAGNETIC SUSCEPTIBILITY

Volume magnetic susceptibilities of the core plugs were measured both on a Bartington bridge (Cape Roberts Science Team, 1999) and on a Kappa bridge (this study). Agreement between the Kappa bridge data and the continuous, whole-core measurements (Cape Roberts Science Team, 1999) is excellent. In contrast, the magnetic susceptibility log needs recalibration. Core-plug and well-log measurements of magnetic susceptibility are highly correlated, so linear regression can be used to calibrate the log data (Tab. 4). Niessen et al. (1998) observed that CRP-1 magnetic susceptibilities tended to be higher in muds than in sands, but the overall correlation between magnetic susceptibility and clay content was weak. Similarly, we detect no correlation between magnetic susceptibility and grain size within our small subset of CRP-2A samples. Brink et al. (this volume) observe that most CRP-2A diamicts have higher magnetic susceptibilities than adjacent sands and muds.

VELOCITY-PRESSURE RELATIONSHIP

CRP-2A measurements

Measurements of velocity at atmospheric pressure are usually not representative of *in situ* velocities, for two reasons: reduced interparticle coupling and microcrack opening. These effects can be reversed by measuring the samples at *in situ* pressures. Modern *in situ* lithostatic pressures for CRP-2/2A sediments are 0.6 - 6.4 MPa.

Brink & Jarrard (1998) measured V_p and V_s as a function of pressure for CRP-1 sediments. Because unlithified sediments such as those from CRP may deform

viscoelastically or break down at fairly modest pressures, Brink & Jarrard (1998) measured velocities of CRP-1 samples on both upgoing and downgoing pressure cycles. A similar approach was taken for four representative samples from CRP-2A. These measurement suites consisted (approximately) of the following pressure steps: 0, 0.69, 1.38, 3.45, 5.17, 6.90, 5.17, 3.45, 1.38, 0.69, and 0 MPa. As is often noted for more lithified rocks, it was not always possible to detect useful V_p or V_s arrivals at the 0 MPa and 0.69 MPa steps, due to insufficient coupling of sample to transducer. To determine the pressure dependence of any viscoelastic or breakdown effects, we alternated each increased-pressure increment with a return to low pressure (0.69 MPa) for remeasurement.

All of the CRP-1 measurement suites of Brink & Jarrard (1998) had demonstrated two major features. First velocities were higher on the decreasing-pressure cycle than on the increasing-pressure cycle. This hysteresis effect was attributed to measurement times that were rapid in comparison with the time needed for establishment of equilibrium pore pressures within the sample. Following a change in confining pressure, fluid may move into or out of the sample pores, and this equilibration of the pore fluid to the pressure change can take a few minutes, particularly for relatively impermeable samples. For the four pilot CRP-2A samples, we found that 10 minutes was enough time to allow the pressure within the samples to equilibrate: little or no velocity change was observed after allowing times from 20 minutes to 24 hours to transpire between several of the consecutive measurements. Consequently, we waited a minimum of 10 minutes between velocity measurements at different pressures for all CRP-2A measurements.

Second, the experimental design of alternating pressure increases with low pressure measurements demonstrated progressive breakdown or destruction of framework stiffness, in response to high pressures. Whereas most CRP-1 samples exhibited substantial breakdown and associated 5-14% velocity reduction at pressures of 10.3-17.2 MPa (Brink & Jarrard, 1998), only the shallowest of the four CRP-2A samples (from 115 mbsf, within the CRP-1 depth range) exhibited this pattern (Fig. 4). In
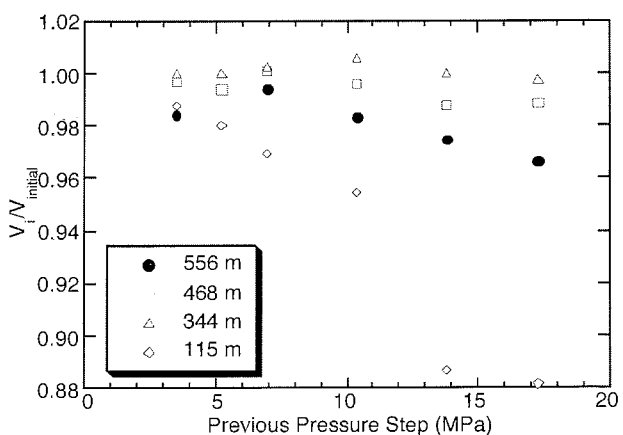

Fig. 4 - Effect of sample exposure to high pressure on velocity measured at 0.69 MPa. $V_{initial}$ is the initial 0.69 MPa measurement of V_p. V_i is a subsequent measurement at 0.69 MPa following the pressure step plotted on the Y axis.

contrast, the three samples from greater depth lacked evidence of sample breakdown (< 2% velocity reduction) even after exposure to high pressures (10.3-17.2 MPa). We conclude that breakdown becomes significant in CRP samples at a pressure that is several times present *in situ* pressure.

Based on these results, velocity measurements for the remaining 38 samples were made in three steps. First, velocity was measured at a differential pressure at or close to the *in situ* differential pressure (based on 10 MPa / km). Samples were not subjected to pressures greater than *in situ* pressure, to avoid the possibility of breaking the sample down before velocity measurements could be accurately made at *in situ* and atmospheric pressures. The second and third steps were at 0.69 MPa and 0 MPa, respectively.

Table 3 lists V_p, V_s, and V_p/V_s for the lowest-pressure and *in situ* pressure steps of all samples that exhibited adequate coupling for useful measurements. Actual measurement pressure, also listed in table 3, is at or near the calculated *in situ* pressure. Occasionally, higher than *in situ* pressures were needed to obtain sufficient transducer coupling for accurate velocity measurement.

Implications for *in situ* velocities

The core-plug measurements provide an independent confirmation of the reliability of the well-log and whole-core measurements. Figure 5 overlays our *in situ* core-plug velocities on a plot of well-log velocities versus depth. For most of the logged interval, core-plug and log velocities are consistent. Within the interval 325-440 mbsf, however, plug velocities may be systematically slightly higher than log velocities. Our data cannot isolate the cause of this possible discrepancy, but a comparison of both datasets to whole-core velocity measurements (Niessen et al., this volume) suggests that some log velocities may be too slow.

Our measurements of velocity versus pressure provide an indication of the likely differences between *in situ* velocities and those measured on continuous cores at laboratory pressure. Figure 6 plots the percentage difference between *in situ* measurements and atmospheric-pressure measurements versus depth, for both CRP-1 (Brink & Jarrard, 1998) and CRP-2A (this study). Nearly all *in situ* velocities are <4% higher than those measured at atmospheric pressure, and most are 0-2% higher. Consequently, the needed adjustment of whole-core velocities to *in situ* conditions is minor; estimates of seismic reflector depths based on whole-core velocities (Cape Roberts Science Team, 1999; Henrys et al., this volume) should be increased by only about 1%.

DIAGENESIS AND COMPACTION HISTORY

SAND AND MUD COMPACTION TRENDS

Figure 7 shows CRP-2A porosities for both sands and muds as a function of depth. Porosities are based on neutron and resistivity logs, calibrated with core-plug porosities as described earlier; lithology is based on core
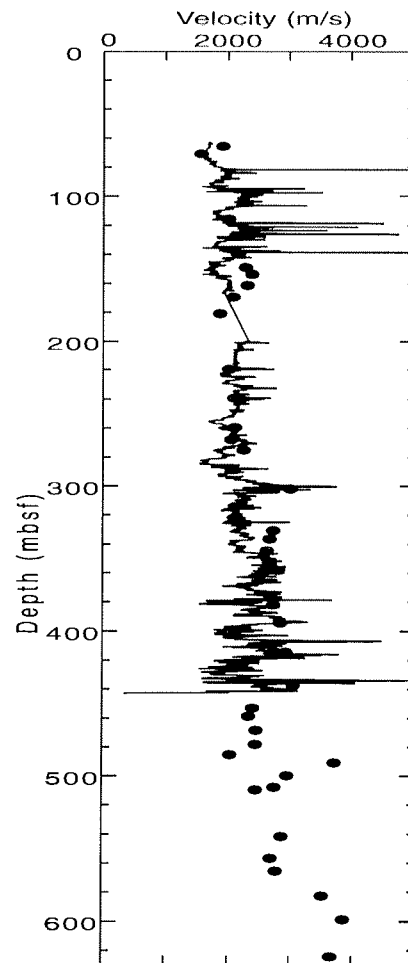

Fig. 5 - Comparison of core-plug velocities to log velocities.

descriptions. As at CRP-1, porosities here are surprisingly similar for sands and muds. Muds appear to be subtly higher in porosity than sands, but porosity variability is so high at a given depth that this pattern is somewhat obscured. Core plugs confirm the dependence of porosity on grain size (Fig. 3): porosity increases with decreasing average grain size, and this effect is stronger than the correlation
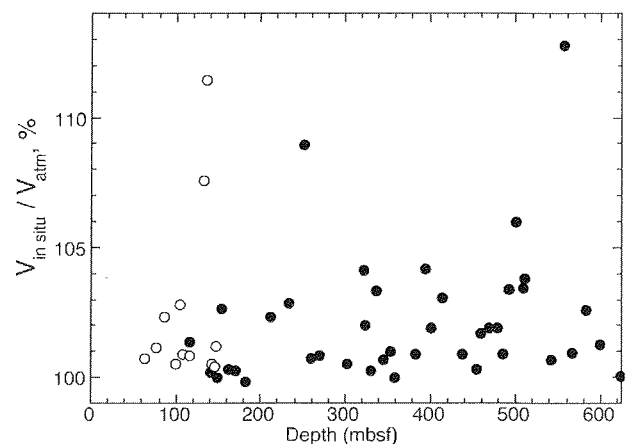

Fig. 6 - Percentage difference between atmospheric-pressure and *in situ* pressure velocities, as a function of depth. Open circles: CRP-1 (Brink & Jarrard, 1998); solid dots: CRP-2A (this study).
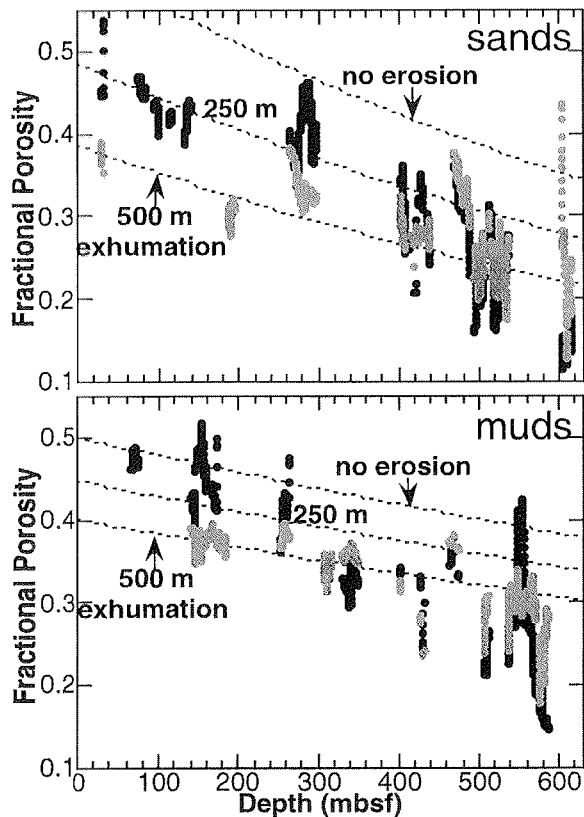
Fig. 7 - Sand and mud porosities versus depth. Black: resistivity-porosity log; grey: neutron porosity log. Solid lines show reference trends for sands (Brückmann, 1989) and muds (Armstrong et al., 1998), assuming 0 m, 250 m, and 500 m of exhumation.

between porosity and depth, at least for the six samples with grain size analyses. Niessen et al. (1998) observed a similar pattern at CRP-1: sands and muds had nearly identical porosity/depth trends, but they were able to detect subtly higher mud porosities than sand porosities.

ESTIMATION OF AMOUNT OF EXHUMATION

Compaction mechanisms and patterns are different for sand and sandstone than for mud and shale. Seafloor porosities of shaly sediments are higher than those of sands and subsequent mechanical compaction is more intense, as the initial "cardhouse" fabric of randomly oriented clay particles is forced into a generally parallel arrangement (*e.g.*, Hedberg, 1936; Magara, 1980). Comparison of the CRP-2 sand and mud compaction trends to empirical trends can provide clues to the compaction history of the site. The similarity of sand and mud porosities ($\phi_{ss} \approx \phi_{sh}$) is typical of burial depths of a few hundred meters, but not of shallower burial ($\phi_{ss} << \phi_{sh}$) or deep burial ($\phi_{ss} >> \phi_{sh}$). CRP-2 sand porosities are systematically lower than predicted by the empirical sand compaction trend of Brückmann (1989) (Fig. 7). Similarly, CRP-2A mud porosities are systematically lower than a reference trend for mudstones and shales of the Taranaki Basin, New Zealand (Armstrong et al., 1998).

Seismic profiles across the CRP-1 and CRP-2/2A sites demonstrate that some exhumation has occurred prior to Quaternary deposition (Cape Roberts Science Team, 1999).

Porosity/depth patterns can be used to estimate amount of exhumation at a well, if a reference porosity/depth trend is available for similar formations in a nearby region with no exhumation. No uneroded reference well is available for CRP-2A, but a rough estimate of exhumation magnitude can be made using reference trends from other regions. Shales, which have an exponential porosity/depth trend, can provide the most reliable exhumation estimates (Magara, 1980) if the local reference trend is well determined, but this is not the case for CRP-2A.

Figure 7 compares CRP-2/2A sand and mud porosities not only to reference trends but also to offset reference trends, assuming 250 m and 500 m of exhumation. The CRP-2A sand porosity/depth pattern is generally consistent with about 250-500 m of exhumation, but discrepancies are nonrandom: the compaction trend is steeper than predicted, so that porosities from 0 to 300 mbsf are compatible with 250 m of exhumation, whereas deeper porosities suggest 400-600 m of exhumation. We attribute this steep compaction trend to the unusually high and strongly depth-dependent cementation observed in CRP-2A cores. Carbonate cementation is subtle in the upper 150 mbsf (Aghib et al., this volume; van der Meer & Davies, this volume); this interval includes sample 115 which showed breakdown at modest pressures. Below 150 mbsf, carbonate cementation is more abundant, increasing with depth and becoming extensive below 400 mbsf (Aghib et al., this volume; van der Meer & Davies, this volume). Correspondingly, carbonate contents increase downhole, from ~1% in the top 100 m to 3-6% below 440 mbsf (Dietrich, this volume). Consequently, the shallow half of the CRP-2A sand dataset is most appropriate for determination of amount of exhumation, leading to a subjective estimate of 250±150 m of erosion. Compared to this 250 m estimate, the anomalously low porosities in the bottom portion of the hole suggest that the unusually intense cementation has reduced porosities by a further 0.05-0.10.

The CRP-2A mud trend, like the sand trend, is steeper than predicted by the reference and exhumed-reference trends (Fig. 7). Again, cementation is the likely explanation. Whereas mud compaction is ordinarily almost entirely mechanical within the top 1 km of burial (Magara, 1980), cementation in the lower part of CRP-2A is evident in muds as well as in sands (Cape Roberts Science Team, 1999; Dietrich et al., this volume; Aghib et al., this volume). Mud porosities for the top half of CRP-2A are compatible with an offset reference trend indicating 300±200 m of exhumation, whereas porosities in the bottom portion of the hole are about 0.1 lower than those based on this prediction. Both the shallow exhumation estimate and deeper cementation estimate for muds are similar to those for sands, but this agreement provides only weak confirmation of the sand-based estimate. Magara's (1980) global compilation of shale compaction trends shows that porosities at a depth of 300 m range from a high comparable to the 0.45 of Armstrong et al. (1998) to a low of about 0.25. Similarly, porosity reduction in the first 600 m of burial can be as low as 0.15 but as high as 0.35-0.45. Thus, one cannot confidently conclude that any exhumation or deep cementation has occurred, based

solely on the mud compaction trend.

Another possible influence on some CRP-2A porosities is glacial overcompaction. For example, CRP-1 sand/silt/mud porosities decrease extremely rapidly with increasing depth, and Niessen et al. (1998) attributed this anomalous trend to glacial overconsolidation of the lower sediments. Although glacial overconsolidation may occur in isolated intervals of CRP-2/2A, it cannot explain the downhole trends in CRP-2 porosities.

The estimate of 250±150 m of exhumation at CRP-2A, based on the sand compaction pattern, is not inconsistent with the estimate of 200-700 m of exhumation (Niessen et al., 1998) at CRP-1, based on a composite sand/silt/mud compaction pattern. The newer estimate is more precise, because the available depth interval at CRP-2A is four times as long as at CRP-1 and because CRP-2A lacks the highly oversteepened compaction trend exhibited by CRP-1.

EXHUMATION EFFECTS ON VELOCITIES: MICROCRACKS?

For unconsolidated sediments, well-log densities are often slightly higher than core-plug and whole-core densities due to rebound, the expansion that cores undergo when removed from *in situ* lithostatic pressures to atmospheric pressure (Hamilton, 1976). Density rebound generally increases from zero at the sea floor to about 100 kg/m³ near 600 mbsf (Hamilton, 1976). Such a pattern is not seen in figure 1, suggesting that rebound is less within CRP-2A than in most other high-porosity sediments. Consequently, when we used core-plug porosities to convert formation-factor and neutron logs to porosity, we did not need to apply any empirical rebound correction to the core-plug data. Velocity rebound usually is larger than porosity rebound, because of both increased porosity and decreased framework stiffness. Consequently, rebound lowers the entire pattern of velocity dependence on porosity (Erickson & Jarrard, 1998b). Because of velocity rebound, nearly all comparisons of laboratory-pressure core-plug velocities to *in situ* log velocities for unconsolidated sediments demonstrate that the core-plug velocities are far too low (*e.g.*, Jarrard et al., 1989, 1993; Fulthorpe et al., 1989). In contrast, velocity rebound at CRP-2/2A is quite low (Fig. 6).

The paucity of velocity rebound (<4%) and the absence of significant porosity rebound are incompatible with normally compacted, unconsolidated sediments. Either these sediments are highly overpressured, which is very unlikely, or rebound must be suppressed by cementation. Hamilton (1971) found that rebound often decreases at depths greater than about 500-600 mbsf because of incipient cementation. At CRP-2A, in contrast, velocity rebound is minor at all depths (Fig. 6), and core descriptions indicate that incipient cementation is present at shallow depths and substantial cementation is evident below 440 mbsf (Cape Roberts Science Team, 1999; Aghib et al., this volume; van der Meer & Davies, this volume).

Stress relaxation, whether caused by exhumation or by core removal from *in situ* pressures, can generate and open microcracks. Most rocks exhibit patterns of increasing V_p

with increasing pressure attributable to closing of microcracks (*e.g.*, Nur, 1971; Bourbié et al., 1987). Initial microcrack porosities of <0.005 are sufficient to cause pressure-dependent velocity variations of 5-50%, indicating that the primary effect of this pressure on velocity is through its impact on frame bulk modulus, not on porosity or density (Walsh, 1965; Nur & Murphy, 1981; Bourbié et al., 1987).

The observed increases of CRP-2A velocities with increasing pressure (Fig. 6) are an order of magnitude smaller than that typical of microcracked rocks. Microcracked rocks exhibit their steepest rate of velocity increase at low-pressure steps comparable to CRP-2A pressures. This flat velocity/pressure behavior, although inconsistent with that of microcracked rocks, is similar to that observed for cemented, uncracked rocks (Bourbié et al., 1987). Again, a cementation signature on CRP-2A velocity behavior appears to be demonstrated.

Another way of detecting any exhumation-induced effects on CRP-2A velocities is to examine the relationship between velocity and porosity. Because of exhumation-induced microcrack opening, the entire velocity/porosity relationship is expected to be lowered substantially (Jarrard & Erickson, 1997; Erickson & Jarrard 1998b). Figure 8 compares CRP-2/2A core-plug velocities, measured at *in situ* pressures, to porosities. In general, the CRP-2A pattern is consistent with the empirical global relationships of Erickson & Jarrard (1998b). The lack of anomalously low velocities, like the flat velocity/pressure behavior, suggests that exhumation-induced microcracking is not present. Because microcracking is expected in association with exhumation, but is not observed today, apparently some of the CRP-2A cementation has occurred subsequently to exhumation.

CONTROLS ON VELOCITY

Velocity is strongly correlated with porosity for the CRP-2A sediments (Fig. 8). Such a relationship is expected from Gassmann's (1951) theoretical model for the controls
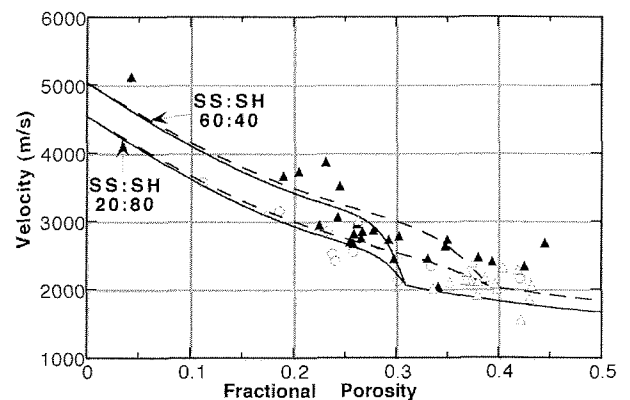
Fig. 8 - Velocity-porosity relationship for CRP-1 and CRP-2A core plugs. Open circles: CRP-1 data (Brink & Jarrard, 1998); open triangles: CRP-2 data from shallower than 325 mbsf; solid triangles: CRP-2A data from deeper than 325 mbsf. Also shown are the global models of Erickson & Jarrard (1998b) for normally compacted (solid lines) and highly consolidated (dashed lines) siliciclastic sediments.

on velocity in porous rocks: porosity is explicitly included in this model, but it implicitly affects velocity also through its influence on frame bulk modulus (Hamilton, 1971), shear modulus (Stoll, 1989), and bulk density. Consequently, siliciclastic rocks and sediments from all parts of the world exhibit a strong dependence of V_p on porosity (Wyllie et al., 1958; Erickson & Jarrard, 1998b).

Despite the high correlation between velocity and porosity, substantial dispersion about the average trend is evident (Fig. 8), implying the presence of some second-order control on CRP-2A velocities. Erickson & Jarrard (1998b) generalized that the second-order control on velocities of siliciclastic sediments depends on porosity: at porosities of less than 30-40%, shale percentage dominates, whereas at higher porosities, consolidation state is more important. Both effects are evident in their empirical trends, shown in figure 8. Because CRP-2A porosities bracket the porosity range at which a transition of second-order controls is expected, both shale percentage and consolidation state may affect CRP-2A velocities.

If the velocity/porosity data of figure 8 are plotted using separate symbols for sands, muds, and diamicts, no lithologic difference in velocity/porosity pattern is detectable. To further investigate the possibility of a lithologic influence on the velocity/porosity pattern, we did grain-size analyses of three pairs of samples. Each pair had the same porosity but significantly different velocity. No correlation between grain size and velocity anomaly is observed. The possibility of some lithologic influence cannot be excluded, but lithology does not appear to be an important direct control on velocity. An indirect influence is probably present: lithology affects porosity, which in turn affects velocity. Niessen et al. (this volume) apply a similar test of lithologic control on CRP-2A velocities, using whole-core data, and find only a subtle association.

Another approach to identifying variables affecting velocity comes from behavior as a function of pressure, as observed in individual plug velocity runs. As previously discussed and observed in figure 6, most samples exhibit little velocity sensitivity to pressure, but some show a few percent change. We arbitrarily divided this continuum of response into "flat" and "pressure-dependent" behavior, then we plotted the two with separate symbol types on the velocity/porosity crossplot, to test three hypotheses: (1) if flat behavior characterizes the more cemented samples, they are expected to lie above the pressure-dependent samples on this crossplot; (2) if pressure-dependent behavior is associated with microcracks, such samples are expected to plot below the other samples; and (3) if pressure-dependent behavior is caused by a plastic deformation of clay-rich samples (Bourbié et al., 1987), then pressure-dependent points are expected to lie above the other points. None of these three hypotheses is confirmed by the CRP-2A data: "flat" and "pressure-dependent" velocity data exhibit no systematic differences on a velocity/porosity crossplot.

Overburden pressure increases framework stiffness by increasing the number and area of intergrain contacts in deeper sediments (Stoll, 1989). Erickson & Jarrard (1998b) examined this effect in downhole logs of unconsolidated

siliciclastic sediments from the Amazon Fan. After removing porosity effects on velocity, they confirmed that pressure affects the velocity of unconsolidated sediments: velocity increased by 0.08 km/s between depths of 100 and 300 mbsf. They were unable to determine, however, whether this pressure influence was elastic or plastic. In other words, is the burial-induced velocity enhancement only present at high pressures, or has burial permanently increased intergrain contacts so that velocity enhancement persists at both high and low pressures?

Figure 8 demonstrates that much of the dispersion in the CRP-2A velocity/porosity pattern is associated with burial depth. CRP-2A samples from deeper than about 325 mbsf have systematically higher velocities, for a given porosity, than samples from above 325 mbsf. The samples from CRP-1, which appear to be anomalously slow when compared to the CRP-2A dataset as a whole (Fig. 8), are very similar in velocity/porosity trend to the shallower CRP-2A data. This agreement confirms the CRP association between velocity/porosity pattern and burial depth, because CRP-1 had a maximum penetration of only 148 mbsf. Niessen et al. (this volume) confirm this observation with their much larger dataset of whole-core measurements.

Unlike the Amazon Fan study of Erickson & Jarrard (1998b), the CRP data permit discrimination between elastic and plastic responses to burial. The elastic velocity response (rebound) of the deeper (>325 mbsf) CRP-2A samples is less than 4% (Fig. 6), or <0.1 km/s, whereas the difference in velocity/porosity trends for shallowly and deeply buried samples is about 0.5 km/s. Consequently, one may conclude that burial has accomplished a permanent increase in intergrain contacts and therefore in framework stiffness. This increase in consolidation is not merely a porosity reduction, because the entire velocity/porosity trend is raised.

The consolidation increase could be either mechanical or diagenetic, because both mechanical compaction and cementation are pervasive at CRP-2A. The velocity enhancement is several times larger than that observed in the mechanically compacted and completely uncemented sediments of Amazon Fan (Erickson & Jarrard, 1998b), so depth-dependent increase in CRP-2A cementation is probably the major cause of the corresponding increase in velocity/porosity pattern. Such an effect is predicted by the model of Erickson & Jarrard (1998b) (Fig. 8). However, although their examination of worldwide velocity/porosity datasets indicated that data from high-consolidation regions were systematically faster than those from normally consolidated localities, they were unable to persuasively isolate the consolidation effect within a single dataset. The CRP-2A data provide that demonstration, because of the dramatic downhole increase in cementation within these high-porosity sediments.

Additional evidence concerning cementation can be found in the V_p/V_s relationship. Figure 9 shows V_p/V_s ratio as a function of porosity. In general, V_p/V_s increases with both greater porosity and greater percentage of clay (Blangy et al., 1993). Figure 9 shows that about half of the CRP-2A V_p/V_s ratios fall within the envelope of data of Blangy et al. (1993), but little or no lithology influence on V_p/V_s ratios is observed. No overall correlation between
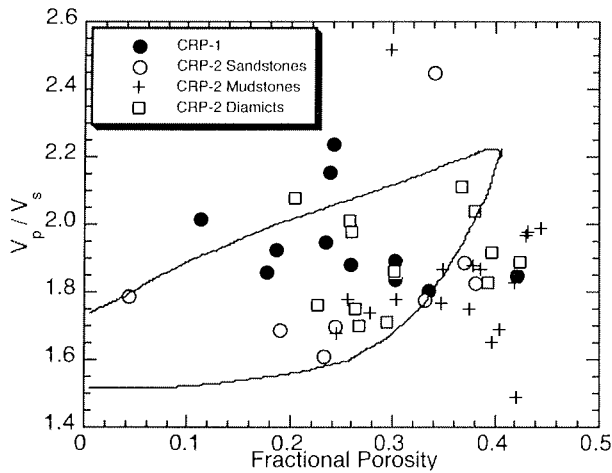
Fig. 9 - V_p/V_s ratio versus porosity for CRP-2A samples, compared to the envelope of data from other regions (Blangy et al., 1993).

V_p/V_s and cementation is apparent: cementation in CRP-2A generally increases with depth, but examination of table 3 shows no systematic pattern of V_p/V_s decrease with depth. However, V_p/V_s ratios of the highest porosity sediments are unusually low, implying enhancement of framework stiffness.

ACKNOWLEDGEMENTS

REFERENCES

Armstrong P.A., Allis R.G., Funnell R.H. & Chapman D.S., 1998. Late Neogene exhumation patterns in Taranaki Basin (New Zealand): evidence from offset porosity depth trends. *J. Geophys. Res.*, **103**, 30269-30282.

Blangy J.P., Strandenes S., Moos D. & Nur A., 1993. Ultrasonic velocities in sands – revisited. *Geophysics*, **58**, 344-356.

Bourbié T., Coussy O. & Zinszner B., 1987. *Acoustics of Porous Media.* Ed. Tech., Paris, 334 pp.

Brink J.D., 1999. Petrophysics and Log-based Sedimentology of the

Cape Roberts Project, Antarctica. Univ. of Utah, *unpubl. M.S. thesis*, 183 pp.

Brink J.D. & Jarrard R.D., 1998. Petrophysics of core plugs from CRP-1 drillhole, Victoria Land Basin, Antarctica, *Terra Antartica*, 5(3), 291-298.

Brückmann W., 1989. Typische Kompaktionsabläufe mariner Sedimente und ihre Modifikation in einem rezenten Akkretionskeil (Barbados Ridge). *Tübinger Geowiss. Arbeiten, Rh. A*, **5**, 1-135.

Cape Roberts Science Team, 1998. Initial Report on CRP-1, Cape Roberts Project, Antarctica. *Terra Antartica*, 5(1), 187 pp.

Cape Roberts Science Team, 1999. Studies from the Cape Roberts Project, Ross Sea, Antarctica, Initial Report on CRP-2/2A. *Terra Antartica*, 6(1-2), 173 pp.

Ehrmann W., 1998. Lower Miocene and Quaternary clay mineral assemblages from CRP-1, *Terra Antartica*, 5(3), 611-612.

Erickson S.N. & Jarrard R.D., 1998a. Porosity/formation-factor relationships for high-porosity siliciclastic sediments from Amazon Fan. *Geophys. Res. Lett.*, **25**, 2309-2312.

Erickson S.N. & Jarrard R.D., 1998b. Velocity-porosity relationships for water-saturated siliciclastic sediments. *J. Geophys. Res.*, **103**, 30385-30406.

Fulthorpe C.S., Schlanger S.O. & Jarrard R.D., 1989. In situ acoustic properties of pelagic carbonate sediments on the Ontong Java Plateau. *J. Geophys. Res.*, **94**, 4025-4032.

Gassmann F., 1951. Elastic waves through a packing of spheres. *Geophysics*, **16**, 673-685.

Hamilton E.L., 1971. Elastic properties of marine sediments. *J. Geophys. Res.*, **76**, 579-604.

Hamilton E.L., 1976. Variations of density and porosity with depth in deep-sea sediments. *J. Sediment. Petrol.*, **46**, 280-300.

Hedberg H.D., 1936. Gravitational compaction of clays and shales. *Am. J. Sci.*, **31**, 241-287.

Jarrard R.D., Dadey K.A. & Busch W.H., 1989. Velocity and density of sediments of Erik Ridge, Labrador Sea: control by porosity and mineralogy. *Proc. Ocean Drill. Program Sci. Results*, **105**, 811-835.

Jarrard R.D. & Erickson S.N., 1997. Sandstone exhumation effects on velocity and porosity: perspectives from the Ferron Sandstone. *Abstracts AAPG Annual Meeting, Dallas.*

Jarrard R. D., Jackson P. D., Kasschau M. & Ladd J. W., 1993. Velocity and density of carbonate-rich sediments from northeastern Australian margin: integration of core and log data. *Proc. Ocean Drilling Program Sci. Results*, **133**, 633-647.

Magara K., 1980. Comparison of porosity-depth relationships of shale and sandstone. *J. Pet. Geol.*, **3**, 175-185.

Niessen F., Jarrard R.D. & Bücker C., 1998. Log-based physical properties of the CRP-1 core, Ross Sea, Antarctica, *Terra Antartica*, 5(3), 299-310.

Nur A., 1971. Effects of stress on velocity anisotropy in rocks with cracks. *J. Geophys. Res.*, **76**, 2022-2034.

Nur A. & Murphy W., 1981. Wave velocities and attenuation in porous media with fluids. *Proc. 4th Int. Conf. on Continuum Models of Discrete Systems*, Stockholm, 311-327.

Sondergeld C.H. & Rai C.S., 1993. A new exploration tool: quantitative core characterization. *PAGEOPH*, **141**, 249-268.

Stoll R.D., 1989. *Sediment Acoustics.* Springer-Verlag, Berlin, 153 pp.

Walsh J.B., 1965. The effect of cracks on the compressibility of rock. *J. Geophys. Res.*, **70**, 381-389.

Wyllie M.R.J., Gregory A.R. & Gardner G.H.F., 1958. An experimental investigation of factors affecting elastic wave velocities in porous media. *Geophysics*, **23**, 459-493.